Lecture 6: Heating of Upper Atmosphere

Basic Facts

- Photosphere T = 6000 k

  Corona T > 10^6 K

  Coronal loops and X-ray bright points have enhanced heating.
- Possible Mechanisms

  -- Mechanical heating: sound (acoustic) waves to shock waves – only explain lower atmosphere

  -- Magnetic heating: for corona, and loops.

  Figs. 1.2 & 6.1, table 6.1 shows the temperature structure of the sun.

Basic Energy Equation

- C = H - R

  Conduction Heating Radiation

  F_c (Downward conduction) = $-\kappa_0 T^{\frac{5}{2}} \nabla T (C = \nabla F_c)$

  At photosphere $C << H \approx R$

  Corona $C \approx H > R$

  A simple numerical:

$$\frac{d}{dz}(\kappa_0 T^{\frac{5}{2}} \frac{dT}{dz}) = \chi n_e{}^2 T^{\alpha} - H$$

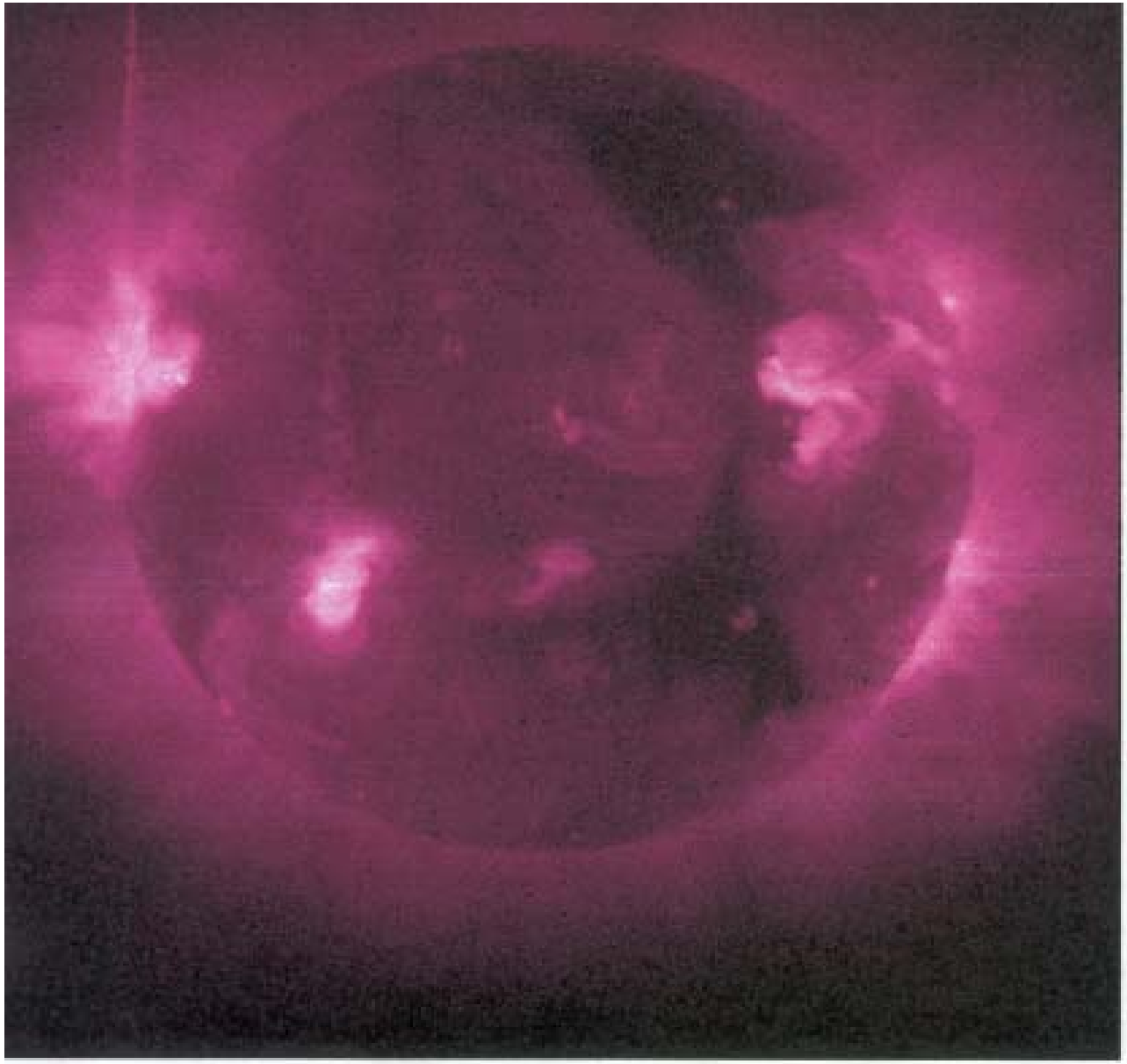

Fig 6.2

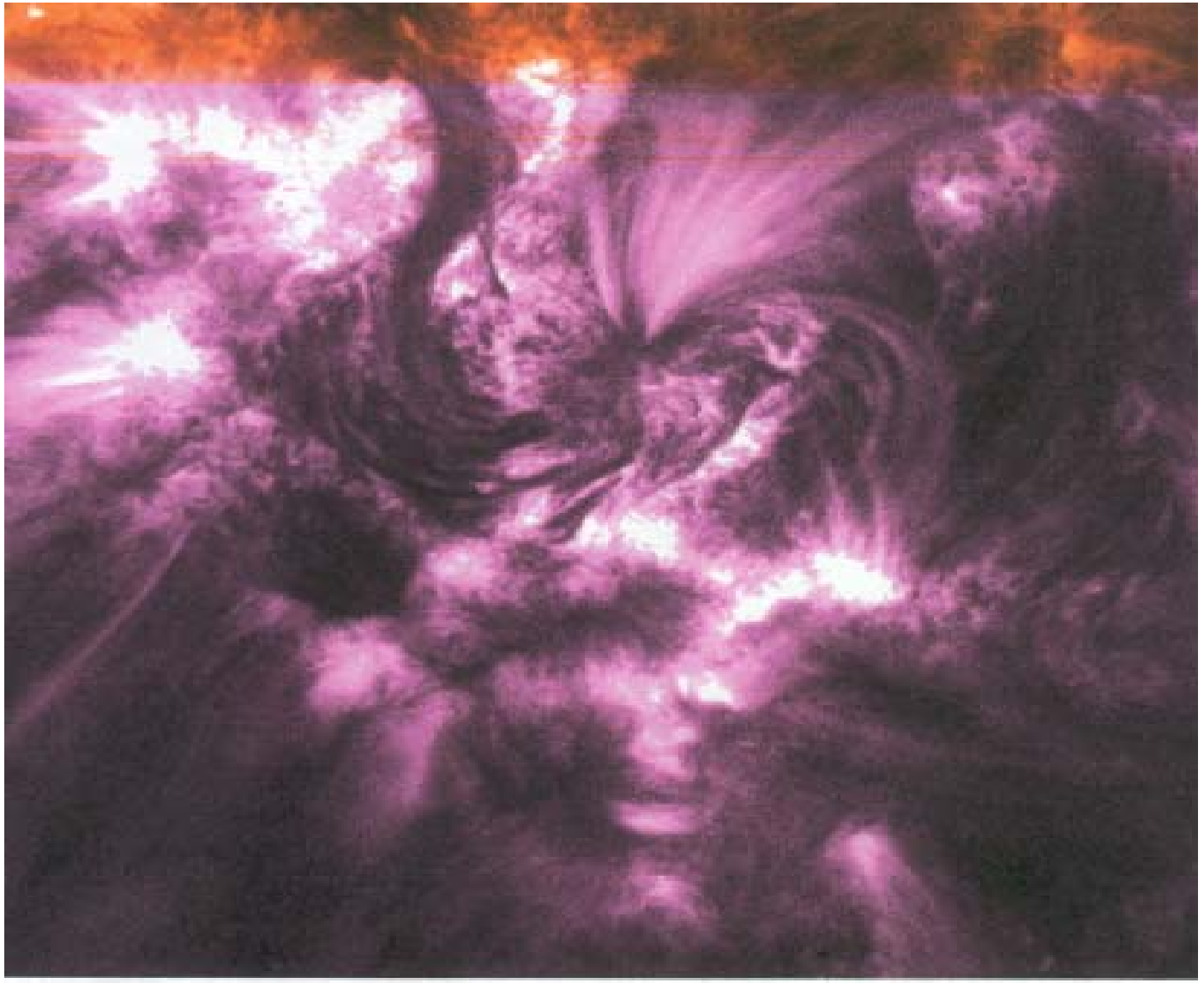

Fig. 6.3

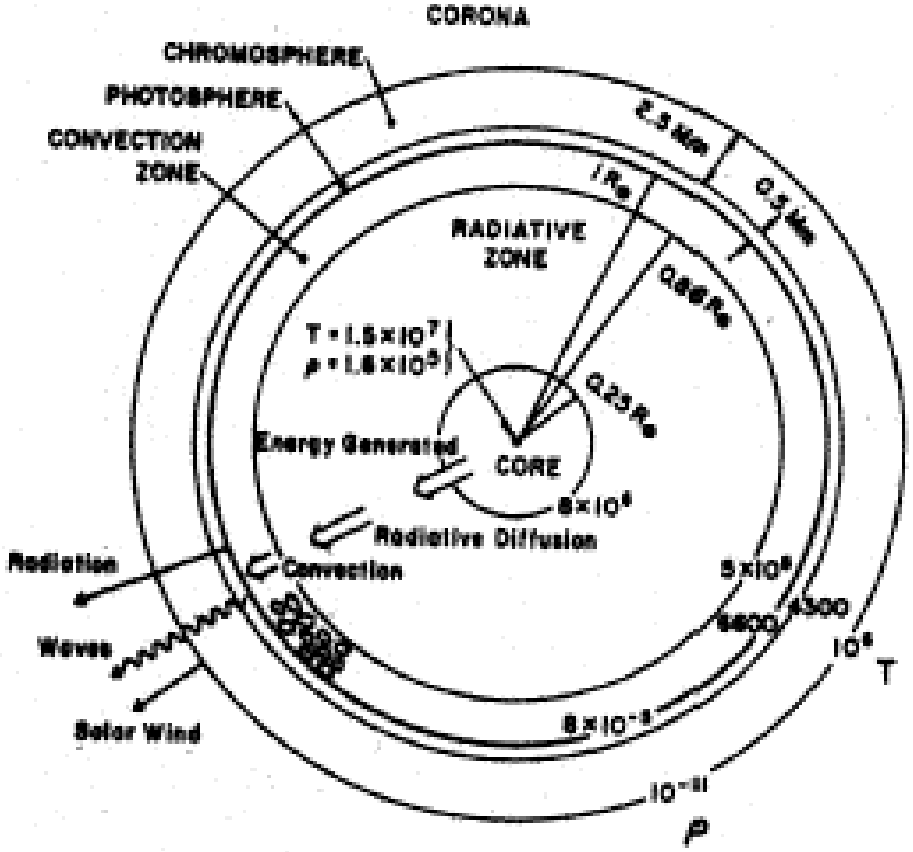

Fig. 1.1. The overall structure of the Sun, indicating the sizes of the various regions and their temperatures (in degrees K) and densities (in kg m^{-3}). The thicknesses of the photosphere and chromosphere are not to scale, and recent models place the base of the convection zone at about 0.7 $R_\odot$ rather than 0.86 $R_\odot$

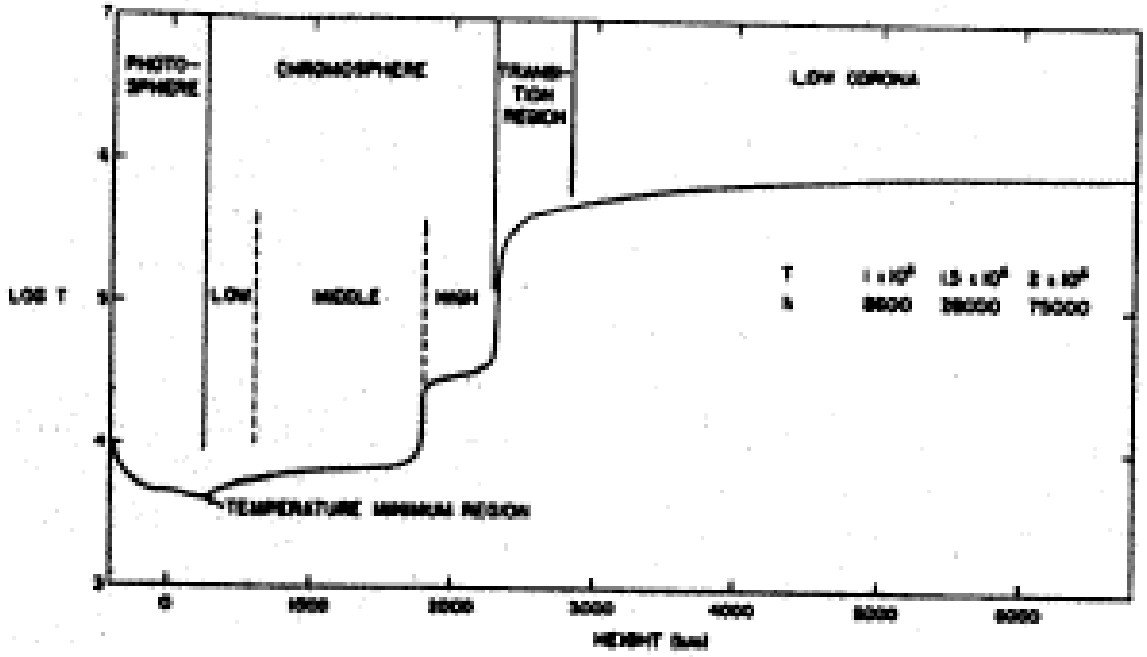

Fig. 1.2. An illustrative model for the variation of the temperature with height in the solar atmosphere (Athay, 1976).

$$\begin{cases} 10^{23}\ \mathrm{m}^{-3} & \text{in photosphere } (n_e \approx 10^{19}), \\ 10^{15}\ \mathrm{m}^{-3} & \text{in transition region,} \\ 10^{12}\ \mathrm{m}^{-3} & \text{at a height of 1 } R_\odot, \\ 10^{7}\ \mathrm{m}^{-3} & \text{at 1 AU,} \\ 10^{6}\ \mathrm{m}^{-3} & \text{in interstellar medium.} \end{cases}$$

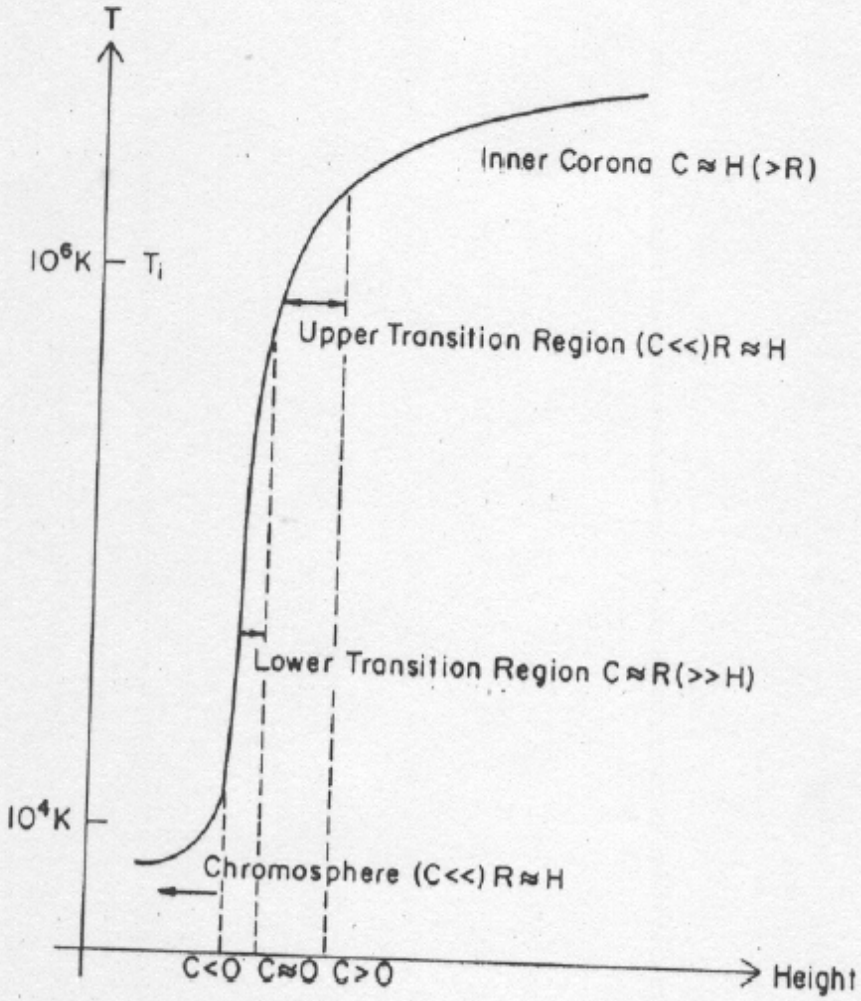

Fig. 6.1. A sketch of the temperature structure in the upper solar atmosphere, indicating the relative roles of conduction (C), radiation (R) and heating (H).

TABLE 6.1.

Energy losses from the upper atmosphere ($1\ W\ m^{-2} \equiv 10^3\ erg\ cm^{-2}\ s^{-1}$)

	Conduction ($W\ m^{-2}$)	Radiation ($W\ m^{-2}$)	Temperature (K)	Pressure ($N\ m^{-2}$)
Quiet region:				
Lower and middle chromosphere		4×10^3		
Upper chromosphere		3×10^2		2×10^{-2}
Corona.	2×10^2	10^2	$1.1 - 1.6 \times 10^6$	
Coronal hole:				
Lower and middle chromosphere		4×10^3		
Upper chromosphere		3×10^2		7×10^{-3}
Corona	6×10	10	10^6	
Active region:				
Lower and middle chromosphere		2×10^4		
Upper chromosphere		2×10^3		2×10^{-1}
Corona	$10^2 - 10^4$	5×10^3	2.5×10^6	

- Hydrostatic equilibrium for fully ionized plasma:

$$\frac{dp}{dz} = -m_p n_e g \qquad p = 2 n_e K T$$

- Effect of magnetic fields:

  Open fields coronal hole: T~10^6K

  Loops: T few x 10^6K

Magnetic Field Can:

- Exerts a force $\vec{j} \times \vec{B}$ to contain plasma with an enhanced pressure.
- Store energy $(\frac{B^2}{2\mu})$, allow additional wave mode and ohmic dissipation (J^2/σ) .
- Channel heat coefficient $\kappa_{//} >> \kappa_{\perp}$, fields act like a thermal blanket.

Fig. 6.3 shows gabrield model – fields concentrated in network boundary of supergrandule, and spread out in coronal – conopy.

$$\frac{d}{ds}(\kappa_{//} A(s) \frac{dT}{ds}) = \chi n_e^2 T^{\alpha} A(s)$$

- Order factors need to be considered.
- Gravitation:

  Turbulent flux: $\rho\upsilon^2$

  Dynamics: spicules.

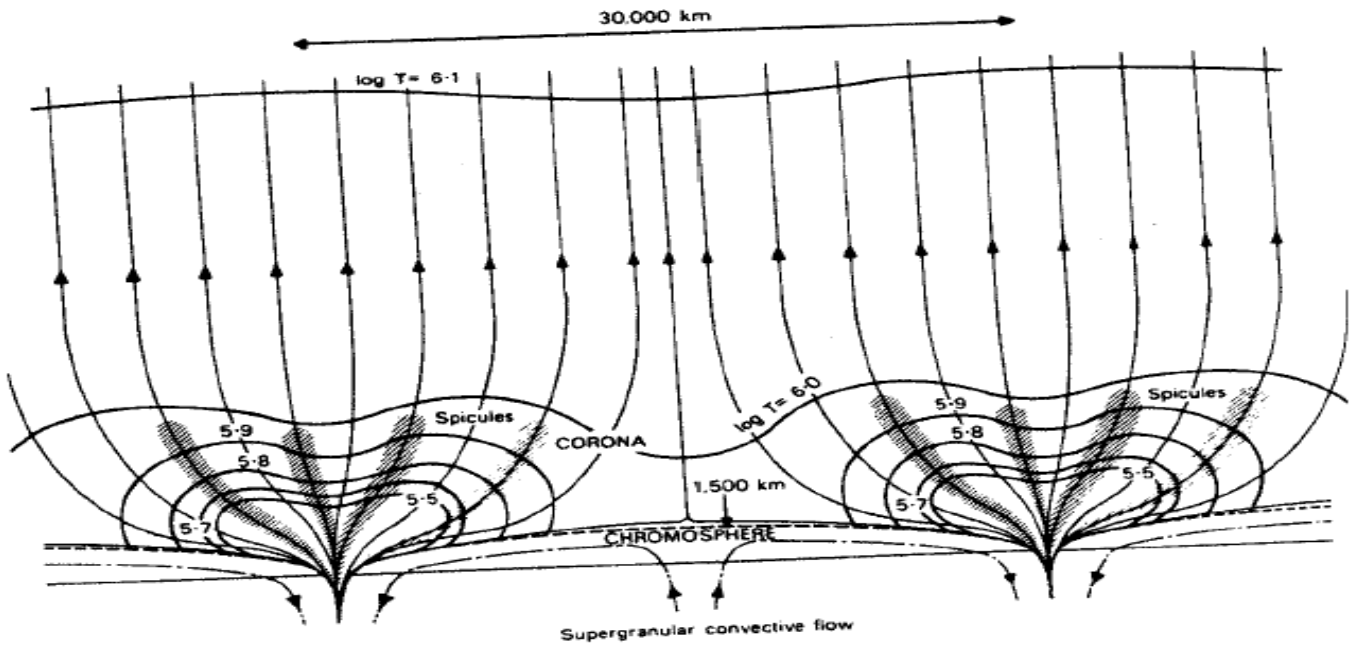

Fig. 6.3. Magnetic field lines and temperature contours for the atmosphere above a supergranule cell in a quiet region (after Gabriel, 1976).

ment with observation for the network width, and the resulting isotherms are sketched in Figure 6.3. By comparison with a plane-parallel model, the effect of the above flux-tube divergence (through $A(s)$) is to increase the temperature gradient at transition-region temperatures and so lower the height at which coronal temperatures are attained. Furthermore, the observed intensities of optically thin lines may be used to derive the differential emission measure ($n_e^2\, T\, \mathrm{d}h/\mathrm{d}T$) as a function of temperature. At temperatures between $10^{5.2}$ and $10^{6.2}$ K, agreement with this emission measure is much better for Gabriel's model than for McWhirter *et al.* (1975)'s previous spherically symmetric models. Below $10^{5.2}$ K there is a need to include heating of amount 2×10^3 W m^{-2}.

Gabriel's model has recently been extended by Athay (1981b), who includes gravitational energy and enthalpy flux but no mechanical heating. With a downflow he obtains good agreement with observations for 3×10^5 K $\leqslant T \leqslant 10^6$ K, and so concludes that there is no need for mechanical heating. In future, there is a need to calculate a wider range of models and to couple the energy balance with a magneto-static force-balance, since the plasma beta is probably of order unity.

6.2.3. Additional effects

Several effects may seriously modify the energy balance in the upper solar atmosphere but they are normally omitted from the models. For example, the waves that may be propagating up from below and heating the atmosphere exert a turbulent pressure, $\langle \rho v^2 \rangle$, which is just the time-average over a wave period of the momentum flux

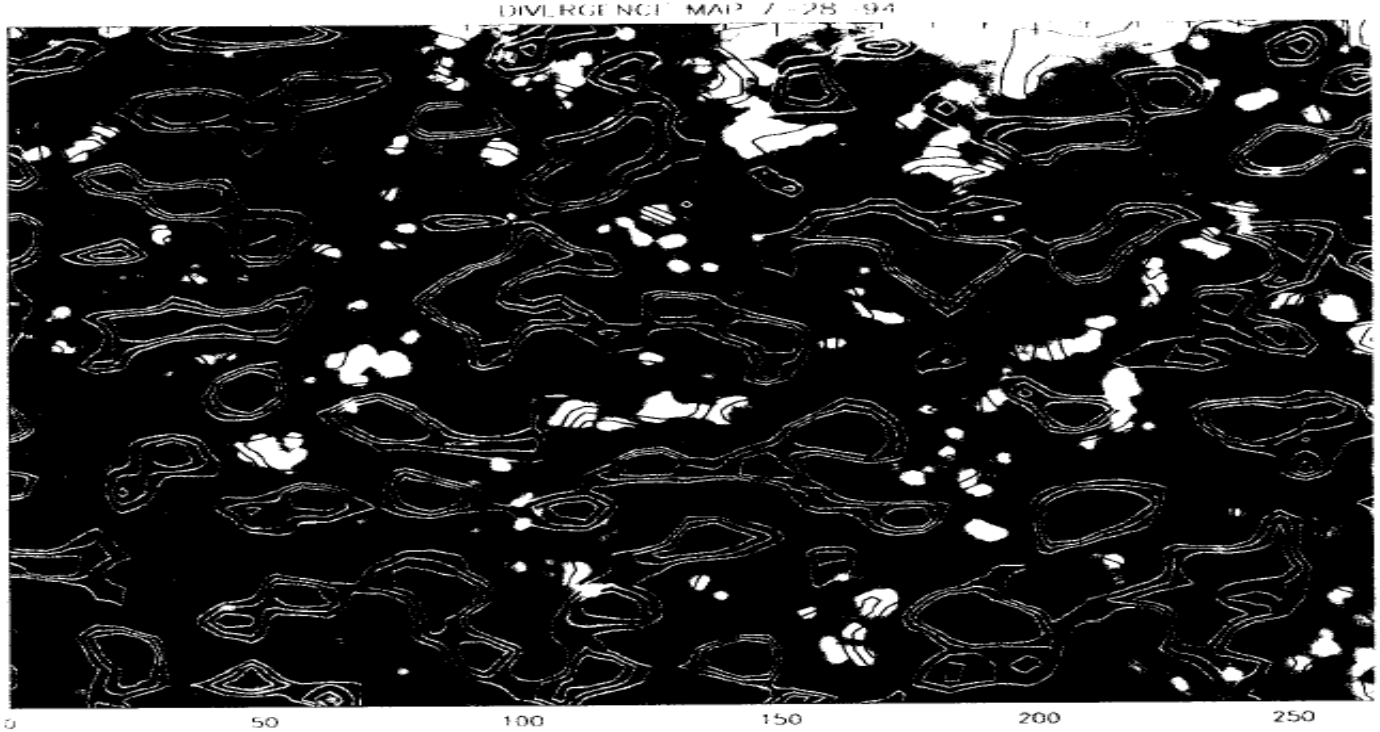

Fig. 3. The divergence map for the velocity fields of the July 28, 1994 region. The dark contours are converging areas and white contours are diverging areas. Contour levels are 0.8, 1.6, and 2.4×10^{-4} s^{-1}. The gray-scale background is the averaged magnetogram.

supergranules – diverging areas correspond to upflow, and converging, downflow. The peak upflow and downflow speeds derived this way are around 50 m s^{-1}, which explains the difficulty of Doppler observations for supergranule vertical velocities. For the same reason that we underestimated the horizontal velocity, we have also underestimated the amplitude of the vertical velocity. The convection flows do not seem to be isotropic; stronger downflows are correlated with stronger magnetic elements. The downflows corresponding to the strong magnetic field areas derived here are the true velocities, and are not caused by the Stokes V asymmetry in the Doppler measurements, as discussed by Stenflo *et al.* (1984).

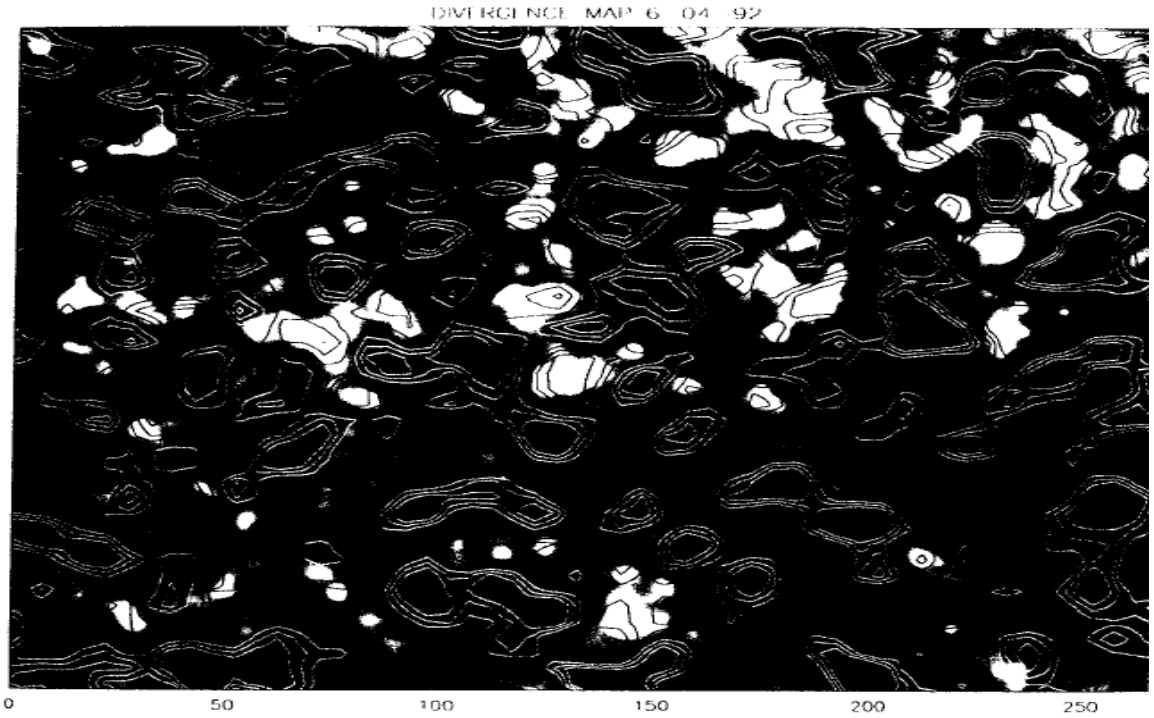

Fig. 4. The divergence map for the June 4, 1992 region.

3.3. ENHANCED AND QUIET NETWORK

The interaction between convection and magnetic fields is a fundamental and interesting problem. It has been found that granular convection motions have been substantially reduced in the area of strong magnetic field areas (Title, Yopka, and Tarbell, 1992). What are the properties of the supergranule cells for different magnetic activity levels? Wang (1988) studied the Dopplergrams measured at different magnetic levels, where he found that the variations of properties of supergranules were within uncertainties. However, the Dopplergrams were taken on different days. Any scale calibration or velocity calibration error could make the results difficult to interpret. In our June 4, 1992 field of view, the magnetic fields are stronger in the right half of the image. Since the images on the two halves were obtained in the same seeing condition, it provides a good opportunity to see if the properties of supergranules depend on the network magnetic fluxes. In Table I we list the key parameters which were derived from the June 4, 1992 observations.

up from the photosphere the temperature drops less rapidly in the regions of enhanced magnetic field, leaving them brighter than their surroundings (Fig. 6.11).

The overall temperature reversal can be observed in the 12μ lines and radio waves. The 812 cm^{-1} (12.32μ) MgI line observed by Brault and Noyes (1983) displays strong double reversal, meaning that the temperature is still dropping at the heights at which the line wings are formed. The emission core indicates that the temperature gradient reverses at the height we see to there. Since the continuum opacity at 12μ is at least 6 times that at 5μ and the absorption line, about 20% deep, the temperature may fall as low as 4000° at $\tau_{5000} = 10^{-6}$. Possibly the temperature reverses at a lower height, but this would require an even higher temperature in the line core, and we should see the core broaden near the limb, which it doesn't.

To study these matters further, we (Popp and Zirin 1987, in preparation)

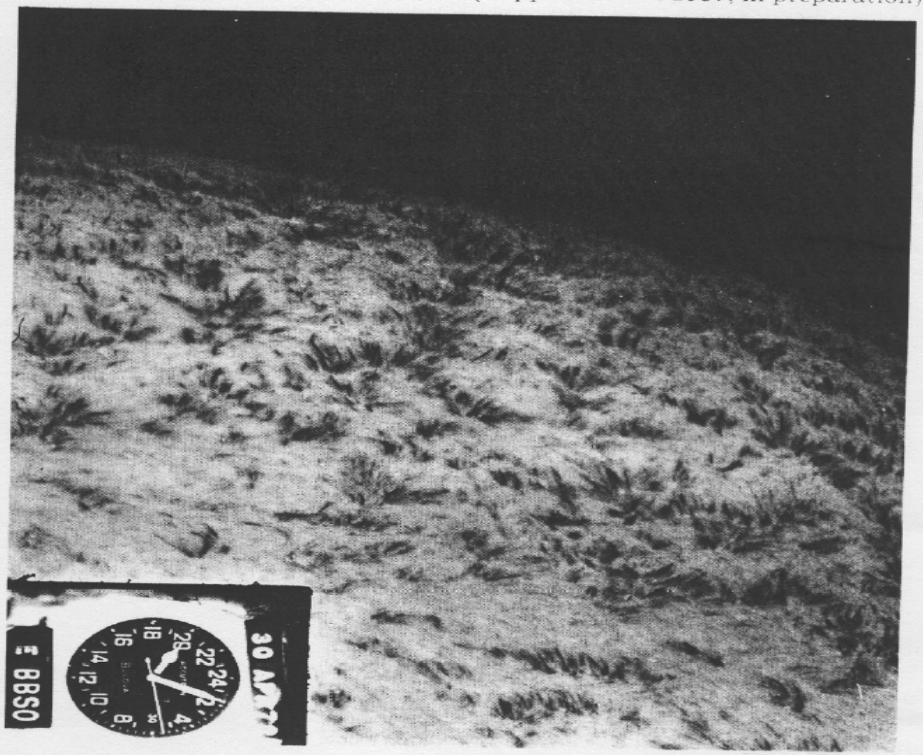

7.3. Spicules in the red wing of Hα. We cannot say much about the time histories because we do not have long enough sequences with such good conditions. (BBSO)

Acoustic Wave Heating

- Acoustic waves are generated near photosphere and to spread to shock waves at a few 100kms, continue to propagate upwards and dissipate energy to balance radiation.
- Shock formation in a continuous uniform atmosphere.

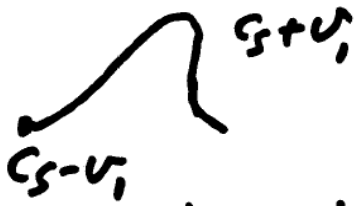

- Distance traveled before shocking is formed:

$$d = \frac{\lambda C_s}{\phi v_1} = \frac{\tau C_s^{\,2}}{4 v_1}$$

- Short wave evolves to shock in a relatively short distance.
- In a vertically stratified atmosphere, distance for shock formation is greatly reduced.

  Density $\rho(z) = e^{-z/\Lambda}, \Lambda$: scale Height

  wave energy $\frac{1}{2}\rho \upsilon_1^{\,2}$ is conserved.

$$\upsilon_1 = e^{z/2\Lambda}$$

e.g. Λ=1000km, initial speed of $\upsilon_1^{(0)} = 0.2km$

υ_1(1000km)=7.5km/s

- In general, shock formation distance:

$$d = 2\Lambda \log_e (1 + \frac{\tau C_s^2}{2(\gamma+1)\Lambda\upsilon_1})$$

$$\gamma = 5/3, C_s = 6km/s, \Lambda = 130km, \upsilon_1 = 0.6km/s$$

$$\tau = 10s, d = 500km$$

$$\tau = 30s, d = 800km$$

Cannot reach Coronal

- Consider a shock wave of frequency:

Flux of energy $F(z) = \gamma \int (\rho - \rho_1)\upsilon dt \Big/ \int dt$

front of shock – 1; rare – 2

$$F(z) = \nu\rho_1(z)C_s(z)^3\bar{\eta}(z)^2 \Big/ 12$$

$$\bar{\eta} = (\rho_1 - \rho_2)\Big/\rho_1$$

Energy dissipation: $\dfrac{dF}{dz} = -\dfrac{\nu z(\gamma+1)\rho_1\eta^3}{12}$

Rate of pressure decrease: $\dfrac{d\rho_2}{dz} = \dfrac{d\rho_1}{dz} - \dfrac{\nu\gamma^2(\gamma+1)\rho_1^2\eta^4}{12F}$

Shock damping length: $d = \dfrac{F}{\dfrac{dF}{dz}} = \dfrac{C_s t_0}{\eta}$

Heating Rate: $H = \dfrac{2}{3}\nu\gamma(\gamma+1)\rho_1(M_1-1)^3$

M_1 match number: $\eta = \dfrac{4(M_1-1)}{C\gamma+1}$

- Short Period Acoustic Waves (10 to 50s)

  Expect to develop weak shock and heat low chromospheres.
- Longer period waves develop into strong shock

Magnetic Heating

- Wave.
- Dissipation.
- Strong (Kilo-gauss) fields in network boundary.
- Footprint motion.
- Magneto-acoustic wave – shock wave.
- When linear treatment is invalid – current sheet.

Propagation and Dissipation of Magnetic Waves

- Fast magnetic-acoustic wave in all directions:
  along fields: max (V_A and C_S)
  cross fields: $\sqrt{(V_A^2 + C_S^2)}$
- Slow magnetic-acoustic wave only in direction close to field.
- Alfren wave group velocity along field.
- When B is below equal-partition, fast mode is the dominant energy carrier. Dissipation of fast shock are the dominant heating mechanism of upper chromospheres.

- Different between acoustic and fast wave:

Shell law

C_s increase, from 10m/s in photosphere to 200km/s in corona.

V_A increase from 10m/s in photosphere to 10^3km/s in corona.

- Acoustic wave can reach corona more easily.

  Fast wave has additional damping – Ohmic dissipation in addition to viscous.

  Time scale for ohmic dissipation is $\tau_d = \frac{\lambda^2}{\eta}$

  η: magnetic diffusivity

  Dumping length: $L_d = V_A \tau_d = \frac{V_A \lambda^2}{\eta} = \frac{V_A^3}{(\eta W^2)}$

Non linear coupling of Aflven waves

- Large flux of Aflven waves are likely generated at supergranule boundary. Aflven wave is likely to dissipate because of its non-linear iteration.

  e.g. Two Alfven waves travel in opposite directions: $W_0=V_AK_0$, $W_1=V_AK_1$
- They can couple into acoustic wave $W_2= C_2K_2$

  $W_2=W_0+W_1$, $K_2=K_0-K_1$

  The coupling is true only if $\frac{W_1}{W_0}=\frac{C_S-V_A}{C_S+V_A}$

  then $W_2=\frac{2W_0C_S}{V_A+C_S}$

- In strong B field, $V_A > C_S$, one Alfven wave can decay into another Alfven wave (W_1,K_1), traveling in the same direction.
- Condition:

$$W_1 + W_2 = W_0$$

$$-K_1 + K_2 = K_0$$

$$W_1 = W_0 \frac{V_A - C_S}{V_A + C_S}$$

$$W_2 = 2\frac{W_0 C_S}{V_A + C_S}$$

- Wave energy flux: $F = \frac{1}{2}\rho \upsilon_1^2 V_A$
- Dissipation length $d = \frac{\tau V_A}{(2\pi)^2}(\frac{V_A}{\upsilon_1})$

- E.g. τ=10s, F=300Wm^2, υ_1=20km/s

  L=2x10^{5}km --- comparable with length of corona loops.
- Open Field (Coronal Holes)

  Long period, τ>10 min.

  F=10Wm^{-2}, drives solar wind

  10s < τ < 5min, F=10^3 to 10^{4}Wm^{-2}

  They are responsible for spicules and coronal heating

- Close Loop:

  Resonant frequencies appear at multiples of $V_A/2L$. L: length of loop;

  e.g. if L=20000km, n=$10^{16}m^{-3,}$

  resonance period = 20s, 10s, 7s, …

- Resonant Absorption of Alfven Wave:

  If ambient medium is non-uniform, a continuous spectrum of Alfven wave may exist. Resonant absorption of such wave at singular surface may exist. They become a means of heating.

- Consider unidirectional field and a plasma pressure which vary with X. $B_0 = B_0(X)\hat{z}$

$$P_0 = P_0(X)$$

Disturbances: $f_1(x,y,z,t) = f_1(x)e^{i(wt-k_y y+k_z z)}$

From 4-60 $\xi(x) = \rho_0(x)\varpi^2 - k_z B_0(x)^2 / u$

For Alfven wave along field:

$$\frac{d}{dx}(\xi(x)\frac{d\upsilon_1 z}{dx}) - k_y{}^2\xi(x)\upsilon_1 x = 0$$

Define: $\varpi_A = \frac{KB}{(u\rho_0)^{\frac{1}{2}}}$ Alfven frequencies

- If $\omega_A = W_A$, second term disappears.

- Singular Surface: -- resonant absorption sheath

  - Plasma energy becomes infinite.

  - Heating occurs.

  - Typically, thickness of the sheath ~ 10 ion Lamor radii.

Magnetic Field Dissipation

- If photospheric motions are slow, and λ Is very long, λ >L, $\tau > T_A = L/A$ wave dissipation is no longer efficient magnetic fields evolve through a series of equilibria which store energy in excess of potential energy. In corona, σ Is so big, ohmic heating is negligible. The only way of dissipation is by current sheets, sheath and filaments which are very thin. Dissipation can be enhanced by turbulence.
- Energy storage rate $\frac{dW}{dt} = \frac{vB^2}{2\mu} L$
- v: photospheric motion speed, twisting a magnetic field of strength B, over area L^2 ohmically dissipate rate: $D = \frac{j^2}{\sigma} L^3$

- If dW/dt>D, excess energy is stored for sudden release, like flare
- If dW/dt=D, the active region reaches a steady state

Typically W=3000 Wm^{-2}, v=100ms^{-1}, B=100G, L=10,000 km, then j=30A/m^2 which requires a ∇B=0.4G/m –- too big

solution: dissipations are through thin sheets – inside the sheets, current j^*, σ^*, thickness l^*

Then: $$D^* = \frac{j^{*2}}{\sigma^*} L^{*2} l^* = \frac{B^2}{\mu\sigma^*} \frac{L^{*2}}{l^*}$$

if $\sigma^*=\sigma$ 10^{-6}, l^* =10m, L^*=1000km will produce similar D^* as above,

So the concepts of current sheet, sheath are introduced

How do current sheet form?

- New flux emergence
- Parker's foot point displacement – nano-flare
- Neutral point and current sheet
  - slow, continuous deformation of 2-D potential fields leads to production of neutral current sheet in perfect conducting limit
  - Initial field: $B_x=y$, $B_y=x$, $z=B_y+iB_x$
  - New configuration $B_y+iB_x=(z^2+L^2)^{1/2}$ current Filament is another special case. it is formed by tearing instability (Fig. 7.13)

6-

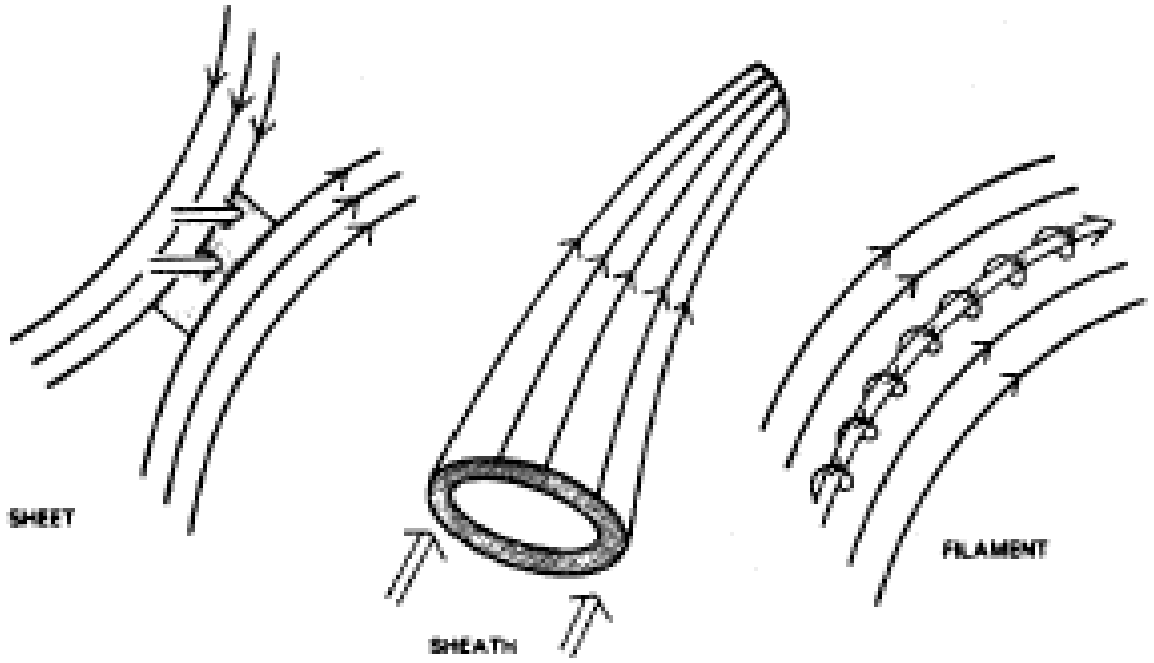

Fig. 6.4. Three geometries for a current concentration in which enhanced magnetic field dissipation may occur. Light arrows label magnetic field lines, whereas large arrows indicate electric current directions.

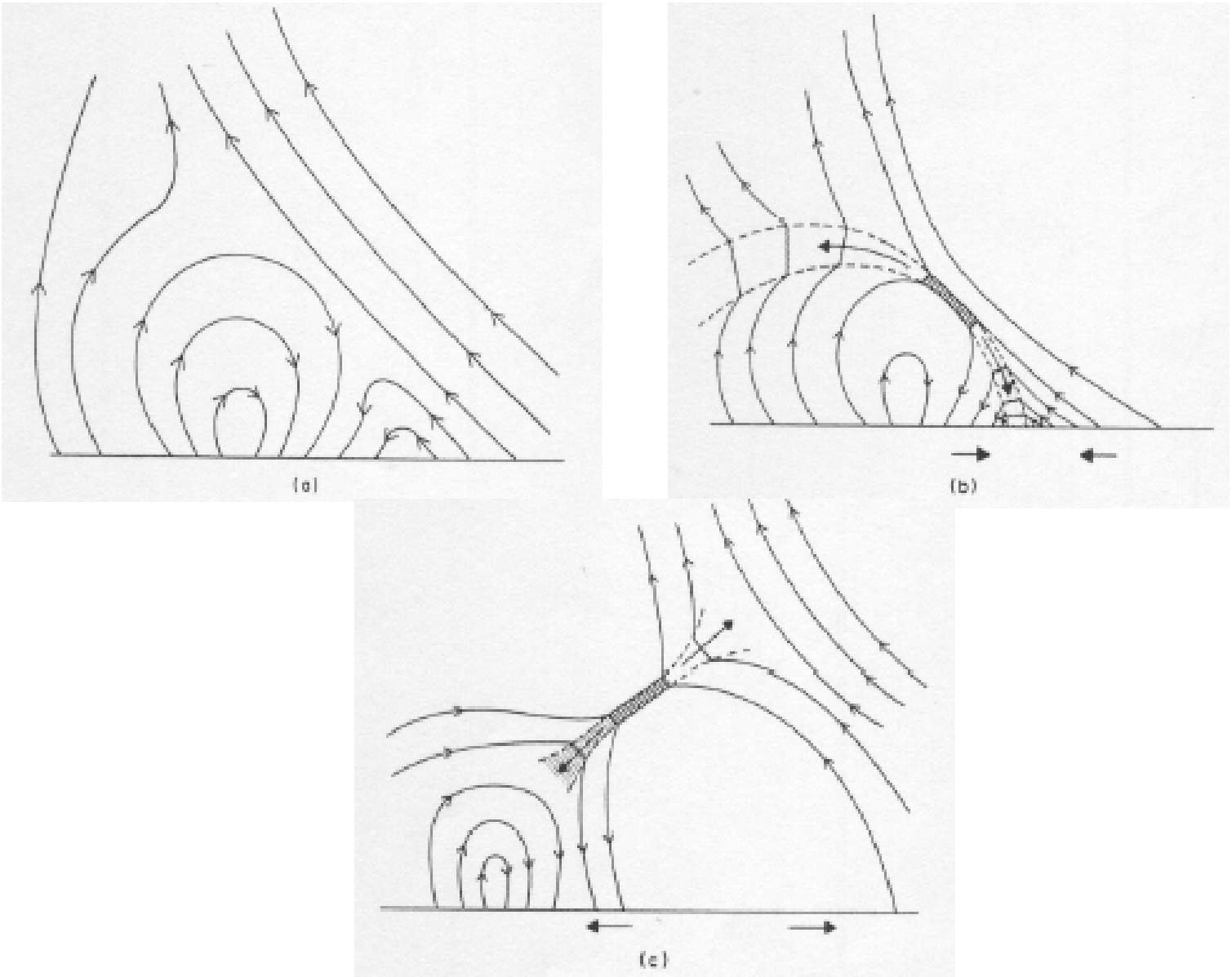

Fig 6.5 Magnetic dissipation due to the relative motion of (a) two neighboring flux tubes when they (b) approach one another or (c) move further apart

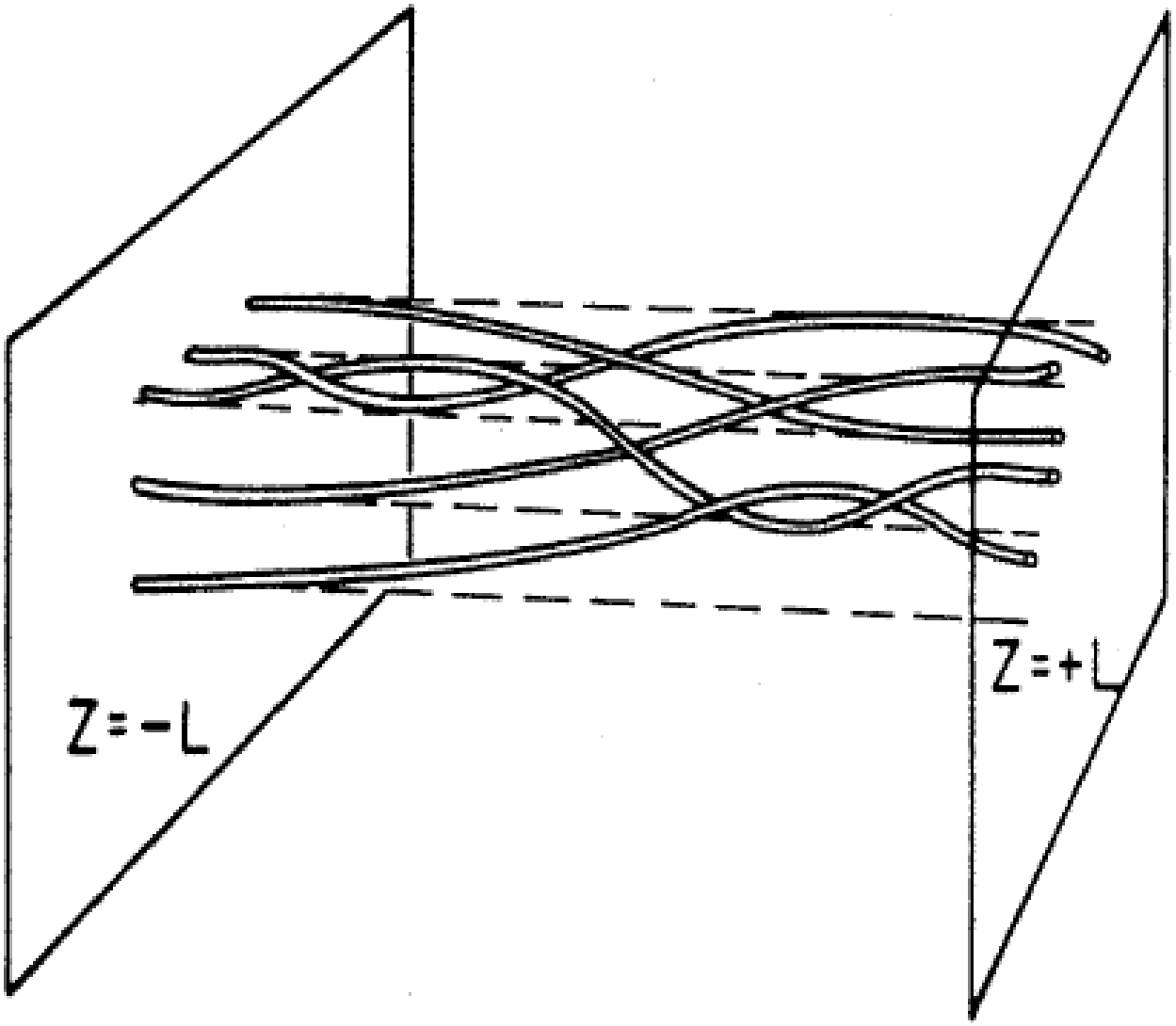

Fig. 6.6. Schematic drawing of the topology of magnetic tubes of force following a displacement of the ends of the tubes where they intersect $z = +L$ (from Parker, 1972).

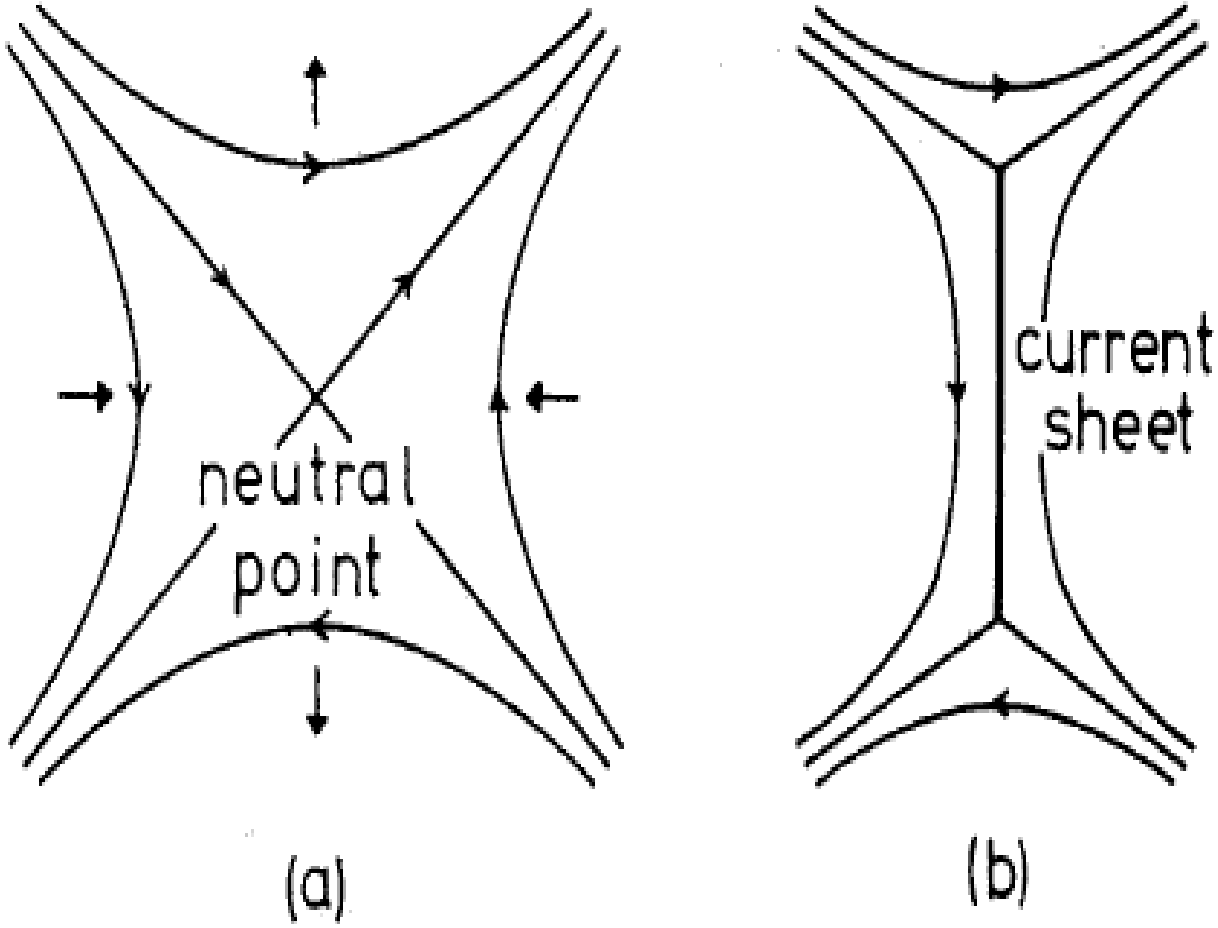

Fig. 6.7. (a) A potential magnetic field near an X-type neutral point. (b) The field produced by the slow motion indicated in (a) by solid-headed arrows. The plasma is assumed perfectly conducting.

Coronal Loops

- Table 6.2 lists properties of 5 different loops.
  - If a loop is in hydrostatic and thermal equilibrium between conduction, radiation and heating then:

$$\frac{1}{A}\frac{d}{ds}(k_0 T^{5/2}\frac{dT}{ds}A) = \chi n_e^2 T^{\alpha} - H$$

$$\frac{1}{Cos\theta}\frac{dp}{ds} = -m_p n_e g, \quad p = 2n_e \kappa T$$

  - A cross section area at distance S from base. Thermally isolated loops requires dT/ds=0 at S=0 under constant P, summit temperature

$$T_1 \sim (pL)^{1/3} \sim H^{2/7} L^{4/7}$$

$$P \sim H^{6/7} L^{5/7}$$

  - Loop can be heated by stretching loop or increasing heating (H)
  - if $P>P_{crit,}$ T decreases, --- cooling (Fig 6.10)

Flows in coronal loops

HEATING OF THE UPPER ATMOSPHERE

Table 6.2

Typical length 2L(×1000km), temperature T(K) and density n(m^{-3}) for the different kinds of coronal loop

	Interconnecting	Quiet-region	Active-region	Post-flare	Simple-flare
2L	20-700	20-700	10-100	10-100	5-50
T	$2\text{-}3\times10^6$	1.8×10^6	$10^4 - 2.5\times10^6$	$10^4\text{ - }4\times10^6$	$\leqslant 4\times10^7$
n	7×10^{14}	$0.2 - 1.0\times10^{15}$	$0.5 - 5.0\times10^{15}$	10^{17}	$\leqslant10^{18}$

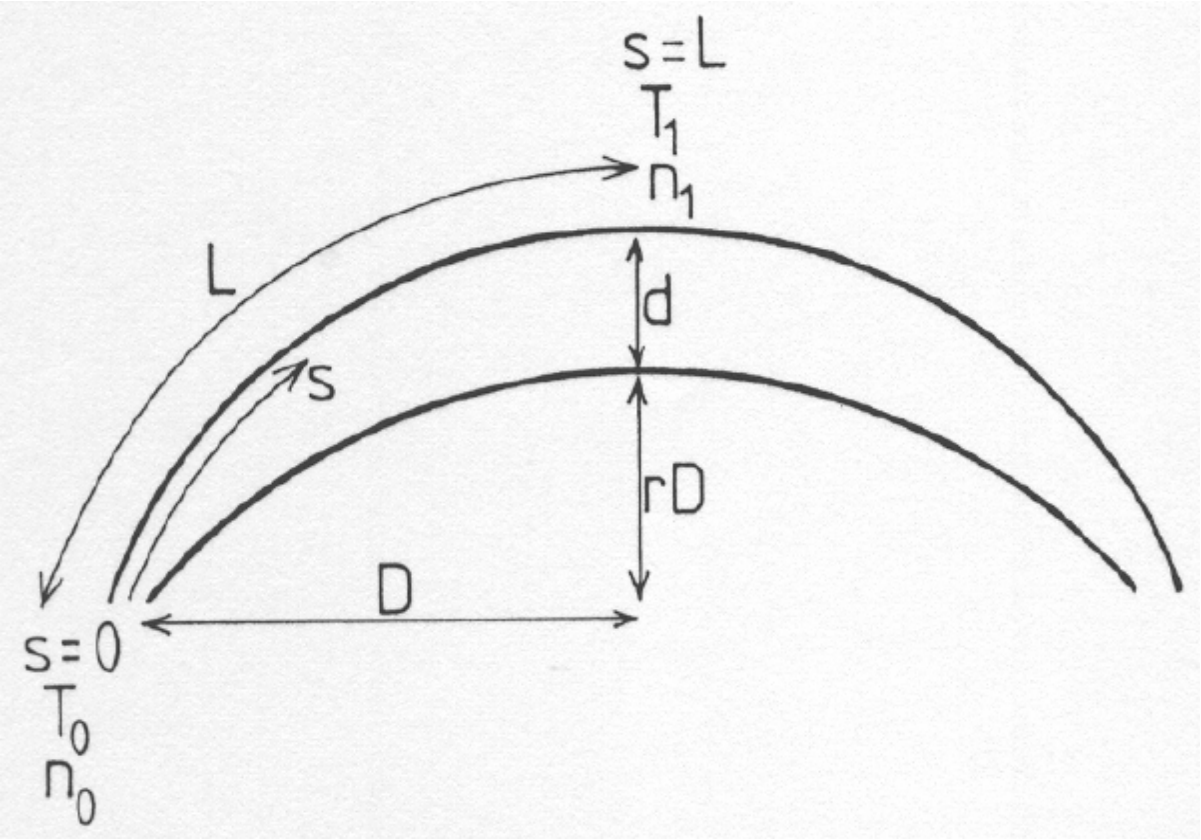

- Fig 6.9 The notation for a symmetric coronal loop of length 2L with temperature T_0 and density n_0 at the footpoint (s=0), and T_1 and n_1 at the summit (s=L). r is the ratio of height to half the base length (D), and d is the ratio of the diameter of loop cross-section at the top to that at the footpoint.

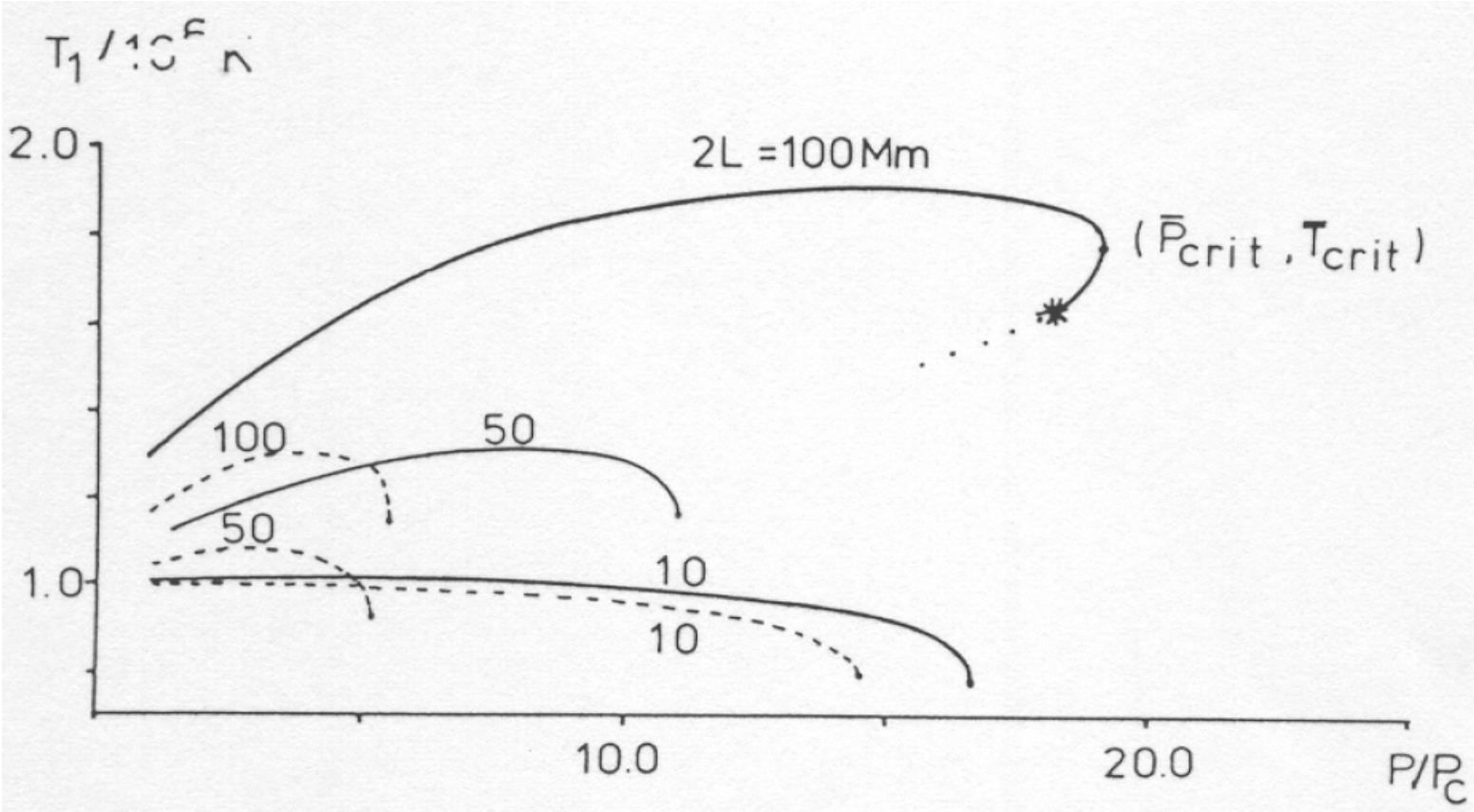

- Fig 6.10 The loop summit temperature(T_1) as a function of the pressure (p) and half-length (L) for a low-lying static coronal loop. p_c is the pressure for a standard plasma of density $5\times10^{14}m^{-3}$ and temperature 10^6K. The solid (or dashed) curves are for mechanical heating ten (or five) times larger than the radiation from the standard plasma. The curves end at critical conditions (p_{crit}, T_{crit}), indicated here for hot loops of length 100000km. The lower unstable solutions are also included for this loop. The star indicates a thermally isolated loop and the dots show oscillatory solutions (form Hood and Priest, 1979a)

- Evershed outflow (6-7 km/s) (Siphon flow)
- Evershed inflow (20 km/s)
  in chromosphere
- Network down flow (0.1 to 2 km/s)
- Surges (20 to 30 km/s) – reconnection
- Spicules (20 to 30 km/s)
- Coronal rain (50 to 100 km/s)
- Evaporation
- Condensation

Homework

Study the paper “An Evaluation of Coronal Heating Models for Active Regions Based on Yohkoh, SOHO, and TRACE Observations” by Aschwanden, Markus J.

2001, Ap.J., 560, 1035

Write a report about its main ideas.